

## Collapse of Charge Ordering in Ru-doped Mono-layered Manganites

Chang Seop Hong<sup>1</sup>, Wan Seop Kim and Nam Hwi Hur\*

Center for CMR Materials, Korea Research Institute of Standards and Science, Yusong, P.O. Box 102, Daejeon 305-600, Korea

<sup>1</sup>Department of Chemistry, Korea University, Seoul 136-701, Korea

(Received 14 December 2002)

The magnetic and transport properties for single crystals of Ru-doped mono-layered manganites  $\text{La}_{0.5}\text{Sr}_{1.5}\text{Mn}_{1-x}\text{Ru}_x\text{O}_4$  ( $0 \leq x \leq 0.1$ ) have been studied using neutron diffraction and magnetization measurements. Temperature dependent magnetization data reveal that with an increase in the Ru concentration the parent charge ordered antiferromagnetic state is gradually destroyed and new ferromagnetic phase evolves. In the low Ru-doped system spin glass behavior is apparent in low temperature region, which is confirmed by ac and dc magnetization measurements. The competing magnetic interaction between Mn/Mn and Mn/Ru couples is the most likely cause of the spin glass transition.

**Key words :** magnetism, charge ordering, manganite, magneto resistance, spin glass

### Introduction

There has been a renewed interest in doped perovskite manganites with the formula of  $\text{R}_{1-x}\text{A}_x\text{MnO}_3$  (R = rare earth ion, A = alkaline earth ion) largely because they display unique magneto transport behavior known as colossal magnetoresistance (CMR) [1]. On the other hand, the CMR behavior accompanied by a ferromagnetic (FM) transition has not been observed yet in the mono-layered manganite with the  $\text{K}_2\text{NiF}_4$  type structure, which thus leads to the less focus of research efforts relative to other layered materials [2]. Nonetheless, the mono-layered phase provides the ample opportunity to explore the interplay among spin, charge, orbital, and lattice in the reduced dimension. For instance, very unusual charge and spin orderings are observed in the half-doped compound  $\text{La}_{0.5}\text{Sr}_{1.5}\text{MnO}_4$  [3]. Interestingly, this charge ordered (CO) state in  $\text{La}_{0.5}\text{Sr}_{1.5}\text{MnO}_4$  is melted by either high magnetic field up to 40 T or photolumination [4, 5]. Moreover, its magnetic and structural properties are very sensitive to the nature of magnetic rare earth ion in the A site as found in the perovskite manganite [6]. Substitution of other transition metal on the Mn site produced drastic doping effects. Particularly, the Cr doping in the CO perovskite changes the parent antiferromagnetic (AFM) state into the metallic

and FM [7]. Many groups have addressed this point with the perovskite system to understand operating mechanism in the Mn site doping [8]. In the mono-layered manganite, however, underlying physics induced by the Mn-site doping has not been extensively investigated.

In this paper we present structural, magnetic, and transport data for single crystals of  $\text{La}_{0.5}\text{Sr}_{1.5}\text{Mn}_{1-x}\text{Ru}_x\text{O}_4$  ( $x = 0, 0.02, 0.05, \text{ and } 0.1$ ). From the comprehensive magnetization and resistivity measurements, we are able to show that the Ru doping suppresses the CO state and induces a new FM phase. Furthermore, we found spin glass behavior appears in the low temperature regime.

### Experimental Section

Single crystals of  $\text{La}_{0.5}\text{Sr}_{1.5}\text{Mn}_{1-x}\text{Ru}_x\text{O}_4$  ( $x = 0, 0.02, 0.05, \text{ and } 0.1$ ) were grown under the oxygen atmosphere using a floating zone image furnace. Crystals cleaved from the resulting boule were cut parallel to the *ab* direction. Electron-probe microanalysis on the Ru-doped crystals confirmed that metal compositions, particularly the Ru to Mn ratio, are consistent with nominal values. The single crystals were crushed into powders for X-ray and neutron diffraction measurements. Neutron powder diffraction data were collected on a high resolution powder diffractometer in KAERI over the angular  $2\theta$  range of  $0^\circ$  to  $160^\circ$  with a step size of  $0.05^\circ$ . Data were analyzed using the Fullprof program. Magnetization and susceptibility measurements

\*Corresponding author: Tel: +82-42-868-5233, e-mail: nhur@kriss.re.kr

**Table 1.** Cell parameters for  $\text{La}_{0.5}\text{Sr}_{1.5}\text{Mn}_{1-x}\text{Ru}_x\text{O}_4$  at 300 K determined by neutron powder diffraction

$x$	$a$ (Å)	$c$ (Å)	$V$ (Å <sup>3</sup> )	$R_{\text{wp}}$ (%)
0.0	3.8611(1)	12.4258(6)	185.25(2)	7.83
0.02	3.8625(1)	12.4410(3)	185.610(6)	9.86
0.05	3.8647(1)	12.4430(3)	185.851(5)	8.33
0.1	3.8673(1)	12.4421(2)	186.084(4)	7.06

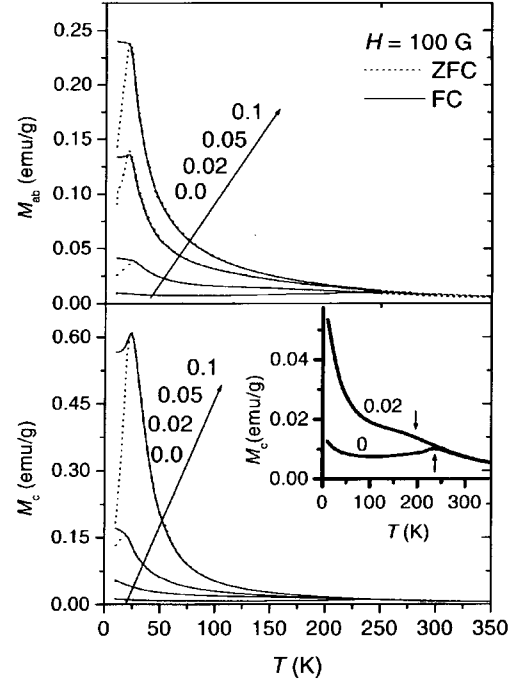
were made on both a MPMS-5 SQUID magnetometer and a PPMS-7 system, where fields are applied parallel to the  $ab$  plane and along the  $c$  axis. Electrical resistivity was measured using the standard four-probe method with and without a magnetic field.

## Results and Discussion

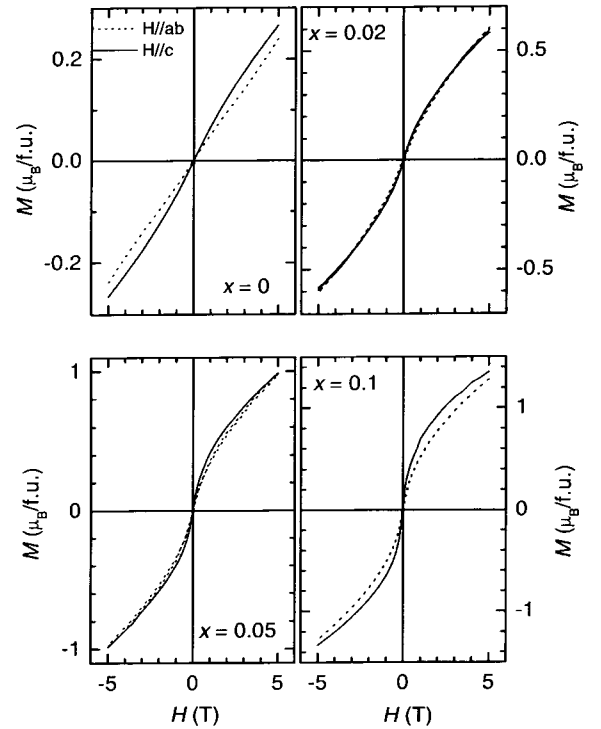
All the samples adopt a tetragonal  $I4/mmm$  symmetry based on Rietveld analysis of neutron powder diffraction data for  $\text{La}_{0.5}\text{Sr}_{1.5}\text{Mn}_{1-x}\text{Ru}_x\text{O}_4$ . The refined structural parameters at 300 K are summarized in Table 1. As the Ru content increases, the unit cell volume tends to expand. This implicates that the Ru ions with the radius of 0.62 Å predominantly replace smaller  $\text{Mn}^{4+}$  ions (0.53 Å) in the Mn sublattice rather than larger  $\text{Mn}^{3+}$  ones (0.65 Å). For  $x = 0.1$  temperature dependent neutron diffraction data were collected at various temperatures. Cell parameters undergo a gradual contraction on cooling, which is analogous to the variation observed in  $\text{Nd}_{0.5}\text{Sr}_{1.5}\text{MnO}_4$  [6]. The diffraction patterns of  $x = 0.1$  at 10 K are perfectly fitted to nuclear peaks, implying that there is no long-range magnetic ordering in the low Ru-doped system.

Figure 1 shows the temperature dependent magnetization curves measured with the applied field parallel to the  $ab$  plane and the  $c$  axis. As can be clearly seen in Fig. 1, the FM contribution is enhanced with increasing  $x$ , implying that the introduced Ru ions induce the FM phase in the AFM matrix. The  $x = 0$  sample has a typical CE-type AFM spin structure that consists of anti-parallel FM zigzag chains. This AFM ground state is gradually destroyed by the Ru doping. The employed  $\text{Ru}^{4+}$  ions appear to induce the FM alignment of four  $\text{Mn}^{4+}$  spins surrounding a  $\text{Ru}^{4+}$  ion. As a result, the FM moment is increased with an increase in the Ru content.

Another notable feature in the  $M(T)$  curves is that the magnitude of magnetic moment with the Ru doping grows more rapidly along the  $c$  axis than in the  $ab$  plane. This behavior is somewhat similar to that found in  $\text{R}_{0.7}\text{Sr}_{1.3}\text{MnO}_4$  ( $R = \text{La}, \text{Pr}, \text{and Nd}$ ) in which the magnetic properties depend on the crystallographic direction as well [9]. This similarity seems natural because the Ru atom also



**Fig. 1.** Temperature dependence of the magnetization for  $\text{La}_{0.5}\text{Sr}_{1.5}\text{Mn}_{1-x}\text{Ru}_x\text{O}_4$  measured parallel to the  $ab$  plane (top panel) and along the  $c$  axis (bottom panel). The applied magnetic field is 100 G. The dotted and solid lines represent the zero-field-cooled (ZFC) and field-cooled (FC) magnetization, respectively. Inset: The expanded view of the  $M(T)$  curves for  $x = 0.00$  and  $0.02$ .



**Fig. 2.** Field dependent magnetization  $M(H)$  data for  $x = 0$  and  $0.1$  along the  $c$  axis and parallel to the  $ab$  plane collected at 5 K.

possesses magnetic anisotropy like magnetic rare earth element. In the Ru-doped system, the Ru spins appear to align toward the  $c$  axis, which in turn will make neighboring Mn spins slant to the  $c$  axis. This anisotropic feature is also observed in the  $M(H)$  plots given in Figure 2. As can be seen in Figure 2, the magnetization along the  $c$  axis is enhanced compared with that parallel to the  $ab$  plane.

Now we turn to discuss the parent CO state originally present in  $x=0$ . As shown in the expanded  $M(T)$  curves for  $x=0$ , given in the inset of Figure 1, magnetization increases with lowering temperature and then decreases upon further cooling. A cusp near 235 K ( $T_{CO}$ ) arising from charge ordering is correlated with the resistivity jump shown in the  $\rho(T)$  curve in Figure 3. A remarkable feature is that this CO state is drastically suppressed by the Ru doping. As displayed in the inset of Figure 1, the cusp is hardly seen in the  $M(T)$  curve of  $x=0.02$ , indicating the collapse of the CO state. Further replacement of Mn with Ru completely destroys the CO phase, which is evidenced by the absence of hump-like transitions in the  $M(T)$  and  $\rho(T)$  curves. Similar behaviors have been observed in perovskite manganites doped with foreign elements, in which a metal-insulator transition occurs simultaneously [7]. This can be understood in terms of the percolation mechanism. In the Ru-doped mono-layered compounds the CO state is also suppressed by doping but the parent-insulating phase is not changed significantly. This might be ascribed to the two dimensional nature of the mono-layered compound. The Ru doping affords the growth of FM domain around the Ru ions as well but the newly formed domains within a layer are difficult to connect to other domains in neighboring layers due to the structural confinement. Interestingly, the Ru-doped sample shows a sizable negative magneto resistance (MR) effect even though the insulating phases are prevailing. The inset of Figure 3 shows the temperature dependence of MR for  $x=0.1$ . Here MR is defined as  $(\rho_H - \rho_0)/\rho_0$  where  $\rho_0$  and  $\rho_H$  stand for the resistivities at 0 and 5 T, respectively. The MR value at 100K is about 60%, which is largely ascribed to the existence of spin glassy state in the low temperature region together with small FM domains induced by the Ru doping [10].

The magnetic properties in the low temperature range for the Ru-doped compounds are of great interest to elucidate underlying physics on the role of Ru in the Mn sublattice. As can be seen in Figure 1, the divergence of the zero-field-cooled (ZFC) and field-cooled (FC) magnetization values is distinctively observed. The cusp temperature in the ZFC curve assigned as  $T_f$  is originated from spin freezing. An interesting feature is that the FC magnetization

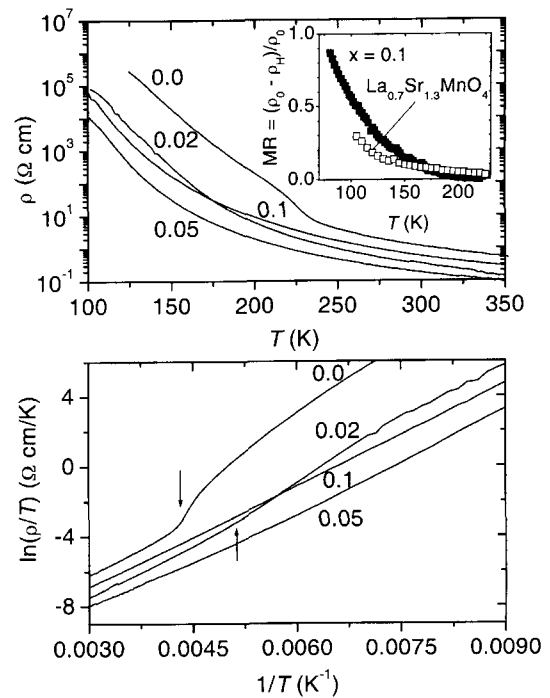


**Fig. 3.** Temperature dependence of in-plane resistivity (top) and logarithmic reduced resistivity (bottom). Inset: temperature dependence of MR for  $x=0.1$ . Arrow indicates the onset temperature of charge ordering.

becomes nearly flat below  $T_f$ , characteristic of canonical spin glass systems [11]. The spin freezing in  $x=0.0$  is apparent at 5 K in the  $ab$  plane while along the  $c$  axis there is no trace of spin freezing down to 2 K. For  $x=0.02$ , however, a dramatic increase in  $T_f$  up to 25 K is found in the  $ab$  plane whereas an advent of spin freezing occurs near 5 K along the  $c$  axis. The increase of  $T_f$  in the Ru-doped samples is associated with the enhanced FM contribution from Ru/Mn couples upon Ru doping. The frustrated spins of the Ru-doped samples might be ascribed to the competing interactions between Ru/Mn and Mn/Mn couples. The spin glassy state in the low temperature regime was also confirmed by ac magnetic susceptibility measurements. Based on the long-time relaxation and aging results of  $x=0.1$ , we have found that re-initialization and multiple memory effect are present in the Ru-doped system, which will be described elsewhere.

In summary, we have investigated the magnetic, structural, and transport properties of single crystals of  $\text{La}_{0.5}\text{Sr}_{1.5}\text{Mn}_{1-x}\text{Ru}_x\text{O}_4$ . An important finding is that the Ru doping destroys charge ordering and induces FM moment. We suggest that the Ru-induced FM moment becomes realized because four neighboring  $\text{Mn}^{4+}$  ions close to a  $\text{Ru}^{4+}$  ion are aligned ferromagnetically. We have also found that the Ru-doped system undergoes spin glass transition in the

low temperature region, which is largely due to the magnetic frustration.

### Acknowledgment

We thank Dr. Y. N. Choi for his kind cooperation. The Creative Research Initiative Program financially sponsored this work.

### References

- [1] S. Jin, T. H. Tiefel, M. McCormack, R. A. Fastnacht, R. and Ramesh, L. H. Chen, *Science* **264**, 413 (1994).
- [2] Y. Moritomo, Y. Tomioka, A. Asamitsu, and Y. Tokura, *Phys. Rev. B* **51**, 3297 (1995).
- [3] B. J. Sternlieb, J. P. Hill, U. C. Wildgruber, G. M. Luke, B. Nachumi, Y. Moritomo, and Y. Tokura, *Phys. Rev. Lett.* **76**, 2169 (1996).
- [4] M. Tokunaga, N. Miura, Y. Moritomo, and Y. Tokura, *Phys. Rev. B* **59**, 11151 (1999).
- [5] T. Ogasawara, T. Kimura, T. Ishikawa, M. Kuwata-Gonokami, and Y. Tokura, *Phys. Rev. B* **63**, 113105 (2001).
- [6] C. S. Hong, E. O. Chi, W. S. Kim, N. H. Hur, K. W. Lee, and C. H. Lee, *Chem. Mater.* **13**, 945 (2001).
- [7] B. Raveau, A. Maignan, and C. Martin, *J. Solid State Chem.* **130**, 162 (1997).
- [8] P. D. Battle, A. M. T. Bell, S. J. Blundell, A. I. Coldea, E. J. Cussen, G. C. Hardy, I. M. Marshall, M. J. Rosseinsky, and C. A. Steer, *J. Am. Chem. Soc.* **123**, 7610 (2001).
- [9] C. S. Hong, W. S. Kim, E. O. Chi, N. H. Hur, and Y. N. Choi, *Chem. Mater.* **14**, 1832 (2002).
- [10] J. Blasco, J. Garcia, J. M. de Teresa, M. R. Ibarra, J. Perez, P. A. Algarabel, C. Marquina, and C. Ritter, *Phys. Rev. B* **55**, 8905 (1997).
- [11] S. Mukherjee, R. Ranganathan, P. S. Anilkumar, and P. A. Joy, *Phys. Rev. B* **54**, 9267 (1996).